732 *Inorg. Chem.* **2011**, *50*, 732–740
DOI: 10.1021/ic101280m

Inorganic Chemistry
Article

Molybdenum Site Structure of *Escherichia coli* YedY, a Novel Bacterial Oxidoreductase

M. Jake Pushie,[†] Christian J. Doonan,[†,‡] Kamila Moquin,[§] Joel H. Weiner,[§] Richard Rothery,[§] and Graham N. George*[,†]

[†]*Department of Geological Sciences, University of Saskatchewan, Saskatoon, Saskatchewan S7N 5E2, Canada, and* [§]*School of Molecular and Systems Medicine, Department of Biochemistry, University of Alberta, Edmonton, Alberta T6G 2H7, Canada.* [‡]*Present address: School of Chemistry & Physics, The University of Adelaide, Adelaide, South Australia 5005, Australia.*

Received June 28, 2010

We report a structural characterization using X-ray absorption spectroscopy of the molybdenum site of *Escherichia coli* YedY, a novel oxidoreductase related to be the sulfite oxidase family of molybdenum enzymes. We find that the enzyme can exist in Mo^{V} and Mo^{IV} oxidation states but cannot be readily oxidized to the Mo^{VI} form. Mo^{V} YedY has molybdenum coordination similar to that of sulfite oxidase, with one Mo═O at 1.71 Å, three Mo−S at 2.39 Å, and one Mo−OH at 2.09 Å, which elongates to 2.20 Å upon reduction to Mo^{IV}, indicating Mo−OH_2 coordination. The Mo^{V} enzyme also possesses a long Mo−O coordination at 2.64 Å, which may be due to oxygen coordination by Asn-45 O_δ, with Mo−O_δ approximately trans to the Mo═O group. A comparison with sulfite oxidase indicates that YedY possesses a much more uniform Mo−S coordination, with a maximum permitted deviation of less than 0.05 Å. Our results indicate that the YedY active site shows considerable similarity to but also important differences from that of reduced forms of sulfite oxidase.

Introduction

The mononuclear molybdenum enzymes catalyze a range of reactions that in most cases involve two-electron redox chemistry coupled to the transfer of an O atom to or from water. The enzymes all possess one or two molybdopterin dithiolene cofactors coordinated to the metal (Figure 1). During the catalytic cycle, the molybdenum cycles between Mo^{VI} and Mo^{IV} oxidation states. Hille[1] has divided the molybdenum enzymes into three families based on the active-site structures of the prototypical enzymes of each family. These are the dimethyl sulfoxide (DMSO) reductase family, the xanthine oxidase family, and the sulfite oxidase family. Sulfite oxidases are widespread and have been identified in mammals, insects, and plants, and closely related sulfite dehydrogenases have been identified in a variety of prokaryotic organisms.[2−5] In animals, the enzyme is localized in the mitochondrial intermembrane space and functions as the final step in the catabolism of sulfur-containing amino acids. In plants, sulfite oxidase is localized in the peroxisome[6] and functions in either sulfite detoxification or regulation of the sulfate pool, whereas the bacterial sulfite dehydrogenases are variously located in the periplasm or cytoplasm.[7] Sulfite oxidase contains two domains: the molybdenum-containing domain and a cytochrome *b* containing domain,[8] which appears to change orientation in solution to facilitate intramolecular electron transfer.[9]

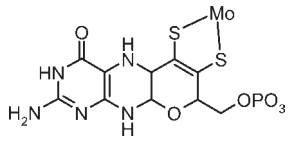

Figure 1. Schematic structure for the molybdopterin molybdenum cofactor.

*To whom correspondence should be addressed. E-mail: g.george@usask.ca.

(1) Hille, R. *Chem. Rev.* **1996**, *96*, 2757–2816.
(2) Rajagopalan, K. V. In *Molybdenum and Molybdenum-Containing Enzymes*; Coughlan, M. P., Ed.; Pergamon Press: Oxford, U.K., 1980; pp 243−272.
(3) Braaten, A. C.; Bentley, M. M. *Biochem. Genet.* **1993**, *31*, 375–91.
(4) (a) Eilers, T.; Schwarz, G.; Brinkmann, H.; Witt, C.; Richter, T.; Nieder, J.; Koch, B.; Hille, R.; Hänsch, R.; Mendel, R. R. *J. Biol. Chem.* **2001**, *276*, 46989–46994. (b) Hille, R. *Structure* **2003**, *11*, 1189–1197. (c) Schrader, N.; Fischer, K.; Theis, K.; Mendel, R. R.; Schwartz, G.; Kisker, K. *Structure* **2003**, *11*, 1251–1263.
(5) (a) Kappler, U.; Bennett, B.; Rethmeier, J.; Schwarz, G.; Deutzmann, R.; McEwan, A. G.; Dahl, C. *J. Biol. Chem.* **2000**, *275*, 13202–13212. (b) Doonan, C. J.; Kappler, U.; George, G. N. *Inorg. Chem.* **2006**, *45*, 7488–7492.
(6) Hänsch, R.; Mendel, R. *Photosynth. Res.* **2005**, *86*, 337–343.
(7) Kappler, U. In *Microbial Sulfur Metalbolism*; Dahl, C., Friedrich, C. G., Eds.; Springer: Berlin, 2007; pp 151−169.
(8) Kisker, C.; Schindelin, H.; Pacheco, A.; Wehbi, W. A.; Garrett, R. M.; Rajagopalan, K. V.; Enemark, J. E.; Rees, D. C. *Cell* **1997**, *91*, 1–20.
(9) Pushie, M. J.; George, G. N. *J. Phys. Chem. B* **2010**, *114*, 3266–3275.

 Published on Web 12/29/2010

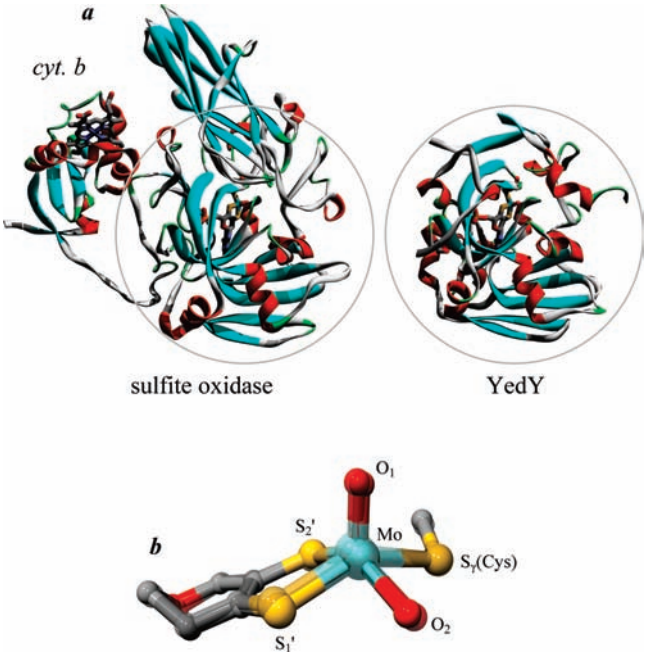

Figure 2. Comparison of the crystal structures of chicken sulfite oxidase and *E. coli* YedY showing (a) the similarity in the polypeptide fold for the molybdenum-containing domain (ringed). Structures were aligned with respect to the atoms of the molybdenum cofactor. Detailed comparison (b) of the molybdenum site structure determined crystallographically for sulfite oxidase (shown as transparent) and YedY (shown as solid). The structures in part b have been rotated relative to those in part a for clarity.

In previous work, the *Escherichia coli* genome sequence[10] was screened for potential mononuclear molybdenum-containing enzymes.[10] This work identified the *yedY* gene, which, together with *yedZ*, forms an operon.[11] The protein YedY contains a twin-arginine translocation signal peptide, which is responsible for targeting the protein for cytoplasmic membrane translocation. Sequence analysis of YedZ indicates six transmembrane segments, and the functional enzyme is thought to be the YedYZ heterodimer, with YedZ providing both a membrane anchor and an electron-transfer partner. YedYZ orthologs are found in a wide variety of bacteria, including a number of important plant, animal, and human pathogens, such as *Erwinia cartovara* (vegetable bacterial soft rot), *Brucella melitensis* (brucellosis), and *Campylobacter jejuni* (human gastroenteritis).[11] From the sequence perspective, YedY aligns poorly with all well-characterized molybdenum enzymes, including sulfite oxidase. YedYZ is thus thought to be a bacterial hememolybdenum enzyme similar to sulfite oxidase, with an as-yet unknown function.[11,12] The crystal structure of *E. coli* YedY has recently been reported at 2.5 Å resolution[11] and shows a protein fold significantly similar to that of the sulfite oxidase domain II (the molybdenum-containing domain; Figure 2).[11,13] The active site shows a single molybdenum coordinated in an analogous fashion to sulfite oxidase, namely, with two S atoms coordinating from the molybdopterin dithiolene at ~2.4 Å, an additional S-donor atom from cysteine 102 at ~2.5 Å, and two O atoms, one at ~2.2 Å attributable to Mo−OH or Mo−OH_2 and the other at ~1.7 Å attributable to Mo=O. The molybdenum coordination sites of YedY and sulfite oxidase are very similar, and the atoms superimpose within crystallographic uncertainties, as shown in Figure 2b. X-ray absorption spectroscopy (XAS) has provided detailed structural information upon the active sites of all of the major classes of molybdenum enzymes, in particular providing an accurate view of the molybdenum coordination unavailable from other techniques.[14,15] We present herein a Mo K-edge XAS study of the active-site structure of *E. coli* YedY and discuss in depth its relationship to that of the sulfite oxidase enzymes.

Materials and Methods

Samples. Recombinant *E. coli* YedY was prepared as previously described.[11,12] All other reagents were obtained from Sigma-Aldrich and were of the highest quality available. Sample preparations were done in 100 mM MOPS/KOH buffer at pH 7.0. To prepare dithionite-reduced samples, 5 mM (final) dithionite with 10 μM (final) methyl viologen was incubated with the sample for 1 min. Samples were transferred to (2 × 10 × 10 mm) lucite cuvettes, which were rapidly frozen in cold isopentane at −140 °C and then transferred to liquid nitrogen prior to XAS data collection.

XAS Data Collection. XAS measurements were conducted at the Stanford Synchrotron Radiation Lightsource, with the SPEAR storage ring containing close to either 100 or 200 mA at 3.0 GeV. Molybdenum K-edge data were collected on the structural molecular biology XAS beamline 9-3 with a wiggler field of 2 T and employing a Si(220) double-crystal monochromator. Beamline 9-3 is equipped with a rhodium-coated vertical collimating mirror upstream of the monochromator and a downstream bent-cylindrical focusing mirror (also rhodium-coated). Harmonic rejection was accomplished by setting the cutoff angle of the mirrors to 23 keV. Incident and transmitted X-ray intensities were monitored using argon-filled ionization chambers, and X-ray absorption was measured as the Mo Kα fluorescence excitation spectrum using an array of 30 germanium detectors.[16] During data collection, samples were maintained at a temperature of approximately 10 K using an Oxford Instruments liquid-helium flow cryostat. For each sample, six to eight scans each of 35 min duration were accumulated, and the energy was calibrated by reference to the absorption of a molybdenum foil measured simultaneously with each scan, assuming a lowest energy inflection point of 20 003.9 eV. The energy threshold of the extended X-ray absorption fine structure (EXAFS) oscillations (k = 0 $Å^{-1}$) was assumed to be 20 025.0 eV.

XAS Data Analysis. The EXAFS oscillations $\chi(k)$ were quantitatively analyzed by curve fitting using the *EXAFSPAK* suite of computer programs[17] as described by George et al.,[18] using ab initio theoretical phase and amplitude functions calculated using the program *FEFF*, version 8.25.[19,20] No smoothing, filtering, or related operations were performed on the data.

(10) Blattner, F. R.; Plunkett, G.; Bloch, C. A.; Perna, N. T.; Burland, V.; Riley, M.; Collado-Vides, J.; Glasner, J. D.; Rode, C. K.; Mayhew, G. F.; Gregor, J.; Davis, N. W.; Kirkpatrick, H. A.; Goeden, M. A.; Rose, D. J.; Mau, B.; Shao, Y. *Science* **1997**, *277*, 1453–1462.
(11) Loschi, L.; Brockx, S. J.; Hills, T. L.; Zhang, G.; Bertero, M. G.; Lovering, A. L.; Weinger, J. H.; Strynadka, N. C. J. *J. Biol. Chem.* **2004**, *279*, 50391–50400.
(12) Brokx, S. J.; Rothery, R. A.; Zhang, G.; Ng, D. P.; Weiner, J. H. *Biochemistry* **2005**, *44*, 10339–10348.
(13) Workun, G. J.; Moquin, K.; Rothery, R. A.; Weiner, J. H. *Microbiol. Mol. Biol. Rev.* **2008**, *72*, 228–248.
(14) George, G. N.; Hilton, J.; Temple, C.; Prince, R. C.; Rajagopolan, K. V. *J. Am. Chem. Soc.* **1999**, *121*, 1256–1266.
(15) (a) George, G. N. *J. Biol. Inorg. Chem.* **1997**, *2*, 790–796. (b) George, G. N.; Hilton, J.; Rajagopalan, K. V. *J. Am. Chem. Soc.* **1996**, *118*, 1113–1117. (c) George, G. N.; Doonan, C. J.; Rothery, R. A.; Boroumand, A.; Weiner, J. H. *Inorg. Chem.* **2007**, *46*, 2–4. (d) George, G. N.; Mertens, J. A.; Campbell, W. A. *J. Am. Chem. Soc.* **1999**, *121*, 9730–9731.
(16) Cramer, S. P.; Tench, O.; Yocum, M.; George, G. N. *Nucl. Instrum. Methods* **1988**, *A266*, 586–591.
(17) http://ssrl.slac.stanford.edu/exafspak.html.
(18) George, G. N.; Garrett, R. M.; Prince, R. C.; Rajagopalan, K. V. *J. Am. Chem. Soc.* **1996**, *118*, 8588–8592.

Electron Paramagnetic Resonance (EPR) Spectroscopy. EPR spectra were recorded on a Varian E109 or a Bruker ESP300E spectrometer equipped with a Bruker ER 4111 ET temperature controller.[12] A modulation amplitude of 0.1 mT was used for all spectra.

Computer simulations were computed using the spin Hamiltonian:

$$H = \beta_e \mathbf{B}\cdot\mathbf{g}\cdot\mathbf{S} + h\mathbf{I}\cdot\mathbf{A}\cdot\mathbf{S} - \beta_N g_N \mathbf{B}\cdot\mathbf{I} \quad (1)$$

where values g_N for ^{1}H and ^{2}H were assumed to be 5.5857 and 0.8574, respectively.

Density Functional Theory (DFT). DFT calculations employed the programs *Dmol*^{3} *Materials Studio*, version 4.1,[21,22] or *Gaussian 03*, revision E.01.23.[23] *Dmol*^{3} calculations used Becke exchange[24] and Perdew correlation[25] functionals for both the potential during the self-consistent-field procedure and the energy. Double-numerical basis sets included polarization functions for all atoms. *Dmol*^{3} calculations were spin-unrestricted, and all electron-core potentials were used, whereas Gaussian calculations implemented an effective core potential for the Mo atom and were spin-restricted, in the case of Mo^{IV}, and spin-unrestricted, in the case of Mo^{V}. Gaussian calculations were performed without symmetry constraints using the hybrid DFT method B3LYP.[23] A mixed basis set approach was employed for geometry optimizations and subsequent harmonic frequency calculations, with an augmented triple-ζ quality version of the LANL2DZ basis set[26,27] used for the Mo atom, 6-31G(d) for the C, O, N, and H atoms, and the larger 6-311+G(d,p) basis set for the S atom. Structures were considered optimized when the change in energy between subsequent optimization steps fell below 0.03 kJ mol^{-1}. Solvation effects were modeled either with the conductor-like screening model (COSMO)[28] in *Dmol*^{3} or with the integral equation formalism polarizable continuum model (IEFPCM),[29−31] with a dielectric value representing water ($\varepsilon = 78.39$). EPR g values were calculated using the program *ORCA*,[32] as described by Klein et al.[33] and employing coordinates derived from the *Gaussian 03* energy minimizations.

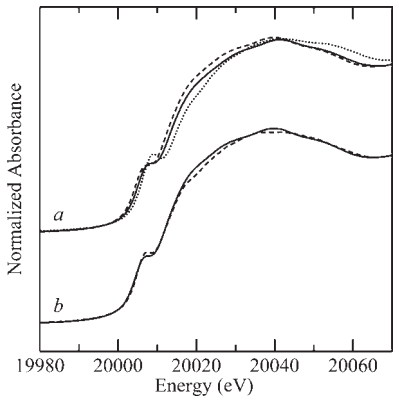

Figure 3. Mo K-edge X-ray absorption near-edge spectra of *E. coli* YedY: (a) as-isolated Mo^{V} enzyme (—) compared to dithionite-reduced Mo^{IV} enzyme (- - -) and oxidized molybdenum(VI) sulfite oxidase (· · ·); (b) reduced Mo^{IV} YedY (—) compared to reduced molybdenum(IV) sulfite oxidase (- - -).

Results and Discussion

XAS. Figure 3 shows the Mo K-edge near-edge spectra of the different forms of YedY. Near-edge spectra are comprised of transitions of the core−electron (Mo 1s in our case) to bound states involving the frontier molecular orbitals of the system, which are sensitive to electronic structure. Figure 3a compares the spectrum of dithionite-reduced YedY with that of as-isolated YedY and oxidized molybdenum(VI) sulfite oxidase. Previous work has established that the as-isolated enzyme is predominantly in the Mo^{V} oxidation state. Unlike sulfite oxidases, the Mo^{V}/Mo^{VI} couple is not observed in redox titrations of YedY; only the Mo^{IV}/Mo^{V} couple (+128 mV at pH 7) is.[12] The dithionite-reduced enzyme will thus be quantitatively in the Mo^{IV} oxidation state and the as-isolated enzyme in the Mo^{V} oxidation state. In the absence of a Mo^{VI} YedY spectrum, Figure 3a shows the expected change in near-edge spectra by comparing the spectra of oxidized sulfite oxidases. As expected from their formal oxidation states, the Mo K-edge near-edge spectrum of the reduced Mo^{IV} enzyme is shifted to lower energy relative to the spectrum of the oxidized Mo^{V} enzyme (Figure 3a) by about 1 eV, which is consistent with the expected redox states of the sites. Both spectra show a distinct shoulder less than halfway up the rising edge, at approximately 20 007.0 and 20 006.2 eV for the Mo^{V} and Mo^{IV} enzymes, respectively. This pre-edge feature is attributed to a formal Mo 1s → 4d(Mo=O) π^* transition[34] and is characteristic of the presence of Mo=O ligation,[35] and its intensity is related to the number of Mo=O ligands.[36−38] The presence of this feature suggests

(19) Rehr, J. J.; Mustre de Leon, J.; Zabinsky, S. I.; Albers, R. C. *J. Am. Chem. Soc.* **1991**, *113*, 5135–5140.
(20) Mustre de Leon, J.; Rehr, J. J.; Zabinsky, S. I.; Albers, R. C. *Phys. Rev. B* **1991**, *44*, 4146–4156.
(21) Delley, B. *J. Chem. Phys.* **1990**, *92*, 508–517.
(22) Delley, B. *J. Chem. Phys.* **2000**, *113*, 7756–7764.
(23) Frisch, M. J.; Trucks, G. W.; Schlegel, H. B.; Scuseria, G. E.; Robb, M. A.; Cheeseman, J. R.; Montgomery, J. A., Jr.; Vreven, T.; Kudin, K. N.; Burant, J. C.; Millam, J. M.; Iyengar, S. S.; Tomasi, J.; Barone, V.; Mennucci, B.; Cossi, M.; Scalmani, G.; Rega, N.; Petersson, G. A.; Nakatsuji, H.; Hada, M.; Ehara, M.; Toyota, K.; Fukuda, R.; Hasegawa, J.; Ishida, M.; Nakajima, T.; Honda, Y.; Kitao, O.; Nakai, H.; Klene, M.; Li, X.; Knox, J. E.; Hratchian, H. P.; Cross, J. B.; Bakken, V.; Adamo, C.; Jaramillo, J.; Gomperts, R.; Stratmann, R. E.; Yazyev, O.; Austin, A. J.; Cammi, R.; Pomelli, C.; Ochterski, J. W.; Ayala, P. Y.; Morokuma, K.; Voth, G. A.; Salvador, P.; Dannenberg, J. J.; Zakrzewski, V. G.; Dapprich, S.; Daniels, A. D.; Strain, M. C.; Farkas, O.; Malick, D. K.; Rabuck, A. D.; Raghavachari, K.; Foresman, J. B.; Ortiz, J. V.; Cui, Q.; Baboul, A. G.; Clifford, S.; Cioslowski, J.; Stefanov, B. B.; Liu, G., Liashenko, A.; Piskorz, P.; Komaromi, I.; Martin, R. L.; Fox, D. J.; Keith, T.; Al-Laham, M. A.; Peng, C. Y.; Nanayakkara, A.; Challacombe, M.; Gill, P. M. W.; Johnson, B.; Chen, W.; Wong, M. W.; Gonzalez, C.; Pople, J. A. *Gaussian 03*, revision E.01; Gaussian, Inc.: Wallingford, CT, 2004.
(24) Becke, A. D. *J. Chem. Phys.* **1988**, *88*, 2547–2553.
(25) Perdew, J. P.; Wang, Y. *Phys. Rev. B* **1992**, *45*, 13244–13249.
(26) Hay, P. J.; Wadt, W. R. *J. Chem. Phys.* **1985**, *82*, 270–283.
(27) Graham, D. C.; Christian, G.; Stranger, R.; Yates, B. F. *J. Comput. Chem.* **2009**, 2146–2156.
(28) Klamt, A.; Schüürmann, G. *J. Chem. Soc., Perkin. Trans.* **1993**, *2*, 799–805.
(29) Cances, E.; Mennucci, B.; Tomasi, J. *J. Chem. Phys.* **1997**, *107*, 3032–3041.
(30) Mennucci, B.; Cances, E.; Tomasi, J. *J. Phys. Chem. B* **1997**, *101*, 10506–10517.
(31) Mennucci, B.; Cammi, R.; Tomasi, J. *J. Chem. Phys.* **1999**, *110*, 6858–6870.
(32) ORCA—an ab initio, DFT and semiempirical SCF-MO package. http://www.thch.uni-bonn.de/tc/orca/.
(33) Klein, E. L.; Astashkin, A. V.; Ganyushin, D.; Riplinger, C.; Johnson-Winters, K.; Neese, F.; Enemark, J. H. *Inorg. Chem.* **2009**, *48*, 4743–4752.
(34) Kutzler, F. W.; Natoli, C. R.; Misemer, D. K.; Donaich, S.; Hodgson., K. O. *J. Chem. Phys.* **1980**, *73*, 3274–3288.
(35) Cramer, S. P.; Wahl, R.; Rajagopolan, K. V. *J. Am. Chem. Soc.* **1981**, *103*, 7721–7727.
(36) Kutzler, F. W.; Scott, R. A.; Berg, J. M.; Hodgson, K. O.; Donaich, S.; Cramer, S. P.; Chang, C. H. *J. Am. Chem. Soc.* **1981**, *103*, 6083–6088.
(37) George, G. N.; Garrett, R. M.; Prince, R. C.; Rajagopalan, K. V. *J. Am. Chem. Soc.* **1996**, *118*, 8588–8592.
(38) Joyner, R. W.; Martin, K. J.; Meehan, P. *J. Phys. C: Solid State Phys.* **1987**, *20*, 4005–4012.

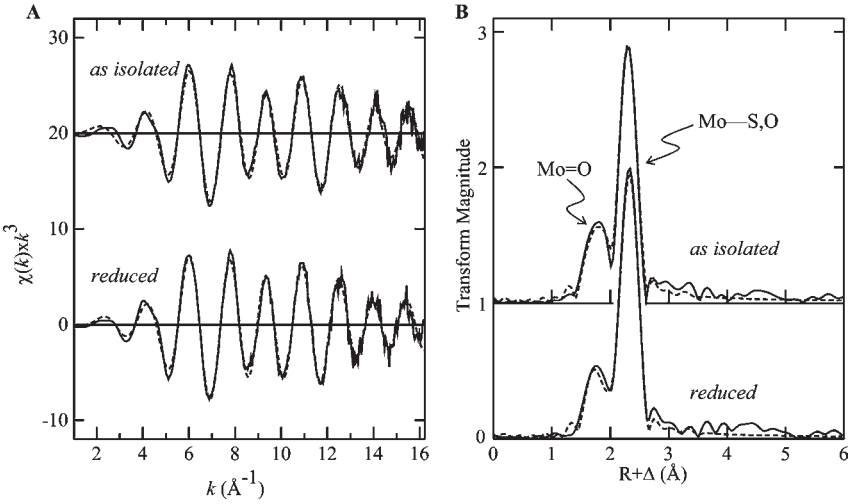

Figure 4. EXAFS curve-fitting analysis of YedY in as-isolated Mo^V and reduced Mo^{IV} forms: (A) EXAFS oscillations and (B) corresponding EXAFS Fourier transforms (Mo−S phase-shift-corrected). Solid lines (—) show the experimental data, while broken lines (- - -) show the best fit. The transform peaks that are indicative of Mo=O and Mo−S contributions are indicated (note that any Mo−O transform peaks will be underneath the Mo−S peak).

the presence of terminal oxo Mo=O coordination in both samples; furthermore, the intensity is lower than that of oxidized dioxomolybdenum(VI) sulfite oxidase (Figure 3a), suggesting that a single oxo ligand is present in YedY. Treatment with oxidizing agents such as 20 mM ferricyanide caused no detectible changes in the near-edge spectrum (not illustrated), but preliminary experiments using a more potent oxidizer, 20 mM hexachlorioiridate(IV), did cause changes, suggesting oxidation, with a significant positive-edge energy shift of almost 2 eV and a near-edge spectrum distinct from other molybdenum enzymes (not illustrated). Further detailed work on the behavior of YedY with such strong oxidants is required, and we will not discuss the potential formation of more oxidized forms further here. Figure 3b also shows a comparison of the near-edges of the fully reduced Mo^{IV} forms of YedY and sulfite oxidase. The spectra are similar but with significant differences, indicating that molybdenum coordination is correspondingly similar but not identical in the two samples. A number of potential YedY activities have been tested by Loschi et al.[11] The enzyme showed no sulfite oxidase activity but did show appreciable reductase activity for sulfoxides such as DMSO and for trimethylamine *N*-oxide, using reduced benzyl viologen as an electron donor. While there is still no evidence as to the physiological substrate, YedY shows reasonable efficiency in the reduction of a number of substrates, although with higher K_m and lower k_{cat} values than enzymes specific to the substrates tested. During the reductase catalytic cycle with substrates such as DMSO, YedY presumably cycles through a Mo^{VI} state, which seems at odds with the redox potentials previously reported. Furthermore, the addition of 5 mM DMSO to as-isolated YedY caused no change in the Mo K near-edge spectrum (not illustrated), indicating that the sample did not change oxidation states. Thus, the nature of the YedY catalytic cycle remains, at this point, somewhat clouded, and improved understanding may need to await the discovery of a physiological role for YedY.

More quantitative structural information on the metal coordination is available from analysis of the EXAFS portion of the spectrum. Figure 4 shows the Mo K-edge EXAFS oscillations of the as-isolated and dithionite-reduced enzyme samples, together with the best fits and EXAFS Fourier transforms. The curve fitting of an as-isolated Mo^V enzyme indicates a single Mo=O interaction at 1.71 Å, three Mo−S at 2.37 Å, and a single longer O atom at 2.08 Å. The active site of the fully reduced Mo^{IV} enzyme is very similar, with one Mo=O at 1.72 Å, three Mo−S at 2.39 Å, and one Mo−O at 2.20 Å. Inclusion of an additional longer-range light backscatterer at about 2.64 Å significantly improved the fit of the Mo^V data, but not the Mo^{IV} data (Table 1). The k range of the data is insufficient to resolve a discrete Fourier transform peak from the interaction, and whether this interaction is present deserves some discussion. The decrease in fit error F when this interaction is included is small, from 0.204 to 0.188, although we estimate that at least 0.1 of this value comes from high-frequency noise in the data (Table 1), and confidence is increased by the fact that the Debye−Waller factor can be fit within chemically reasonable bounds. The question of whether observed improvements in the EXAFS fit are significant when discrete frequencies are not observed is not trivial because statistical significance tests are not applicable when two models that have been independently refined are compared.[14,38,39] However, the bond length of the 2.64 Å interaction was found to be stable to different starting values, and examination of the covariance matrix indicated no significant correlation with other variables in the fit. Moreover, examination of the search profile, in which the value of fit error F is plotted as a function of variables in the refinement, indicates a very well-defined minimum (Figure 5), and a similar plot for the fully reduced Mo^{IV} enzyme shows no equivalent minimum (not illustrated). We note that EXAFS cannot distinguish between atoms of similar atomic number;[40,41] thus, while Mo−S and Mo−O have very different phases and cannot readily be confused, Mo−O

(39) Sachs, L. *Applied Statistics*, 2nd ed.; Springer-Verlag: New York, 1984.
(40) George, G. N.; Pickering, I. J. In *Brilliant Light in Life and Materials Sciences*; Tsakanov, V., Wiedemann, H., Eds.; Springer: Dordrecht, The Netherlands, 2007; pp 97−119.
(41) Doonan, C. J.; Stockert, A.; Hille, R.; George, G. N. *J. Am. Chem. Soc.* **2005**, *127*, 4518–4522.

Table 1. Selected YedY EXAFS Curve-Fitting Results[a]

	Mo=O			Mo−S			Mo−O				
	N	*R*	σ^2	*N*	*R*	σ^2	*N*	*R*	σ^2	ΔE_0	*F*
as-isolated	1	1.714(3)	0.0020(2)	3	2.369(2)	0.0024(1)	1	2.08(2)	0.008(2)[b]	−15.8(6)	0.205
	2	1.710(2)	0.0051(3)	3	2.370(2)	0.0024(1)				−15.3(7)	0.226
	1	1.714(3)	0.0020(3)	2	2.362(3)	0.0024(2)[c]	1	2.09(2)	0.009(2)[b]	−15.5(6)	0.204
				1	2.392(3)	0.0024(2)[c]					
	1	**1.715(2)**	**0.0020(3)**	**3**	**2.373(2)**	**0.0024(2)**	**1**	**2.10(2)**	**0.008(2)[b]**	**-14.3(6)**	**0.188**
							1	**2.64(1)**	**0.0031(6)**		
reduced	**1**	**1.718(3)**	**0.0021(2)**	**3**	**2.390(1)**	**0.0024(1)**	**1**	**2.20(1)**	**0.003(1)[b]**	**-11.3(5)**	**0.206**
	1	1.718(3)	0.0024(2)	3	2.392(1)	0.0024(1)	1	2.20(1)	0.003(1)[b]	−11.2(5)	0.214
							1	2.73(2)	0.006(2)[b]		
oxidized SO[d]	2	1.727(2)	0.0022(1)	3	2.424(2)	0.0039(1)					
reduced SO[d]	1	1.723(2)	0.0018(1)	2	2.35(2)	0.0034(7)	1	2.297(2)	0.0020(2)		
				1	2.41(2)	0.0035(4)					

[a] Coordination numbers, *N*, interatomic distances *R* (Å), Debye−Waller factors σ^2 (Å^2), and threshold energy shift ΔE_0 (eV). Values shown in bold represent the best fits obtained for a particular species. Values in parentheses are the estimated standard deviations obtained from the diagonal elements of the covariance matrix. We note that these are precisions and are distinct from the accuracies, which are expected to be larger (ca. ±0.02 Å for *R* and ±20% for *N* and σ^2), and that relative accuracies (e.g., comparing two different Mo−S bond lengths) will be more similar to the precisions. The amplitude scale factor, otherwise known as the many-body amplitude reduction factor, or S_0^2, was defined by fitting data from a number of model compound species as 1.05. The fit-error function *F* is defined as $[\sum k^6[\chi(k)_{calc} - \chi(k)_{expt}]^2/\sum k^6\chi(k)_{expt}^2]^{1/2}$, where the summations are over all data points included in the refinement. We estimate that high-frequency noise contributes approximately 0.1 to *F* for both data sets. In all cases the *k* range of the data fitted was from 1.0 to 16.2 Å^{-1}. [b] This parameter was constrained to within chemically reasonable bounds.[15] [c] These Debye−Waller factors were found to be highly correlated in the fit so they were held to a common value and constrained within chemically reasonable bounds.[15] [d] Values for sulfite oxidase (SO) were taken from a previous high-resolution EXAFS study,[42] where oxidized and reduced refer to enzymes containing formally Mo^{VI} and Mo^{IV}, respectively.[42] Experimental and analysis differences between this earlier study and the present one mean that the nonstructural parameters ΔE_0 and *F* are not directly comparable with our values for YedY, and these have been therefore omitted from the table.

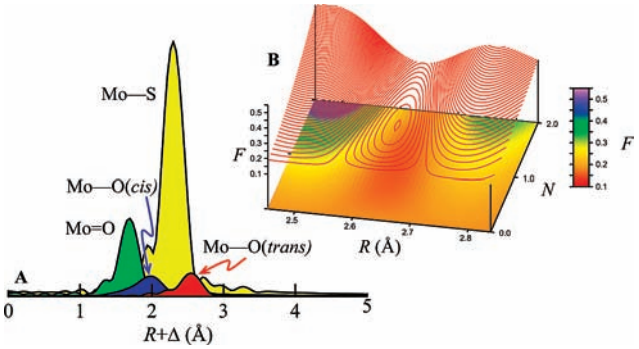

Figure 5. (A) EXAFS Fourier transform showing the four different components detected in curve-fitting analysis of Mo^V YedY, computed using the best-fit values given in Table 1. (B) Search profile showing the minimum for the 2.64 Å Mo−O in Mo^V YedY.

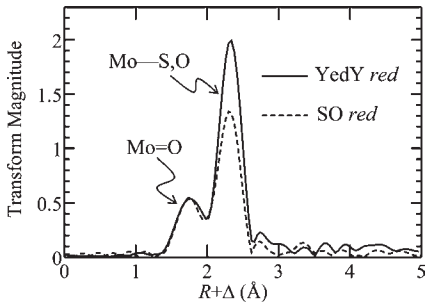

Figure 6. Comparison of the EXAFS Fourier transforms (Mo−S phase-shift-corrected) of Mo^{IV} YedY (—) and reduced molybdenum(IV) sulfite oxidase (- - -) showing the significantly more intense Mo−S interaction for YedY.

and Mo−N (for example) are sufficiently similar that these atoms cannot be distinguished by EXAFS alone. Thus, we conclude that the Mo^V form of YedY contains an unexpectedly long Mo−O or Mo−N coordination and that this is not present in the Mo^{IV} form of the enzyme.

Although they are expected to be present, the 2.08 and 2.20 Mo−O EXAFS of Mo^V and Mo^{IV} YedY are partly in-phase with the intense Mo−S EXAFS, and because of this, a higher degree of uncertainty is associated with the derived structural parameters (Table 1). As a consequence of this, the Mo−S and Mo−O Debye−Waller factors were observed to be highly correlated in the refinement and restraints were imposed upon the Mo−O value to ensure that it remained within chemically reasonable bounds (Table 1).

For both reduced and oxidized enzyme samples, the determined Debye−Waller factor for the Mo−S interaction is low at 0.0024 Å^2 (Table 1), and this can be used to estimate the distribution of Mo−S bond lengths. In this regard, YedY is different from sulfite oxidase, and this is illustrated by Figure 6, which compares the EXAFS Fourier transforms of the fully reduced Mo^{IV} forms of the two enzymes. A significantly larger Mo−S peak is observed for YedY, which is due to the lower Mo−S Debye−Waller factor. The Debye−Waller factor σ^2 is defined as the mean-square deviation from the average bond length *R* and has both vibrational and static components, such that $\sigma^2 = \sigma_{vib}^2 + \sigma_{stat}^2$. To a first approximation, σ_{vib}^2 for a single absorber−backscatterer pair can be estimated using the expression for a diatomic harmonic oscillator:

$$\sigma_{vib}^2 = \left(\frac{h}{8\pi^2\mu\nu}\right)\coth\left(\frac{h\nu}{2kT}\right) \qquad (2)$$

where ν is the vibrational frequency of the bond-stretch vibration, μ is the reduced mass, *k* is Boltzmann's constant (not to be confused with the photoelectron wave vector *k*), and *T* is the temperature. The contribution σ_{stat}^2 arises from structural disorder in the bond lengths (in this case, three Mo−S) differing by less than the EXAFS resolution $\Delta R \approx \pi/2k$ (where *k* is the extent of the data in Å^{-1}). For *N* backscatterer atoms separated

from the absorber atom by an average distance R and individually by R_i, the static component is given by

$$\sigma_{\text{stat}}{}^2 \approx \frac{1}{N}\sum(R_i - R)^2, \quad \text{where} |R_i - R| \leq \pi/2k \qquad (3)$$

Using ν for known compounds and eq 2, we have previously estimated values for $\sigma_{\text{vib}}{}^2$ of 0.0020 Å^2 for Mo−S bonds at the temperature of measurement.[14] Thus, the value of $\sigma_{\text{stat}}{}^2$ is approximately 0.0004 Å^2, indicating that the maximum deviation in the Mo−S bond length possible is 0.047 Å for two identical short and one long Mo−S, or alternatively 0.020 Å for three different and equally separated Mo−S. The protein crystallography analysis suggests that one Mo−S (that of the bond to the cysteine 102 S_γ) is about 0.1 Å longer than the other two. While the resolution of protein crystallography makes this a tentative conclusion, the EXAFS clearly indicates that the Mo−S bonds are of surprisingly uniform bond length for both Mo^V and Mo^{IV} oxidation states. This constitutes a significant difference compared with sulfite oxidase, where the reduced Mo^{IV} enzyme shows two Mo−S distances at 2.35 Å and one at 2.41 Å.

The nature of the two Mo−O linkages is also of significant interest. The shorter of these is the atom that is the candidate group for the putative oxygen exchange with the substrate, assuming that YedY is indeed an oxidoreductase. In xanthine oxidase, we have identified the catalytically transferred O atom as being bound to a Mo atom as hydroxyl with a bond length of 1.98 Å,[38,42] whereas in sulfite oxidase, we find that it is water at 2.30 Å. Examination of the Cambridge Structural database[43] indicates typical Mo−OH and Mo−OH_2 bond lengths of 2.01 and 2.24 Å, respectively. In agreement with this, DFT gives values for hydroxide and water of 2.08 and 2.34 Å, respectively. The YedY crystal structure clearly shows electron density in the active-site pocket adjacent to the Mo−O group, which was assigned to be urea from the crystallization liquor,[11] but alternatively may be residual substrate or product. The nearest atom of this active-site-bound molecule is separated from the O atom by more than 3 Å and thus is outside the range of covalent bonding. Taken together, the Mo−O bond lengths of YedY suggest that the Mo^V and Mo^{IV} forms have Mo−OH and Mo−OH_2 coordination, respectively (Table 1).

Mo^V EPR Spectroscopy. The Mo^V EPR spectrum of YedY (Figure 7) is unusual for a molybdenum enzyme.[12] The **g** tensor is unusually anisotropic, and YedY shows a higher g_z than other enzyme-related Mo^V species at 2.030,[44] which is even larger than the well-known very rapid Mo^V EPR signal from xanthine oxidase, although with lower **g** anisotropy.[45] Kirk and co-workers have also performed preliminary analysis of the ^{95,97}Mo YedY hyperfine using the magnetic isotopes that are naturally present and have presented a simulation that superficially resembles the satellite spectra.[44] However, significant differences are also apparent, so that the derived spin

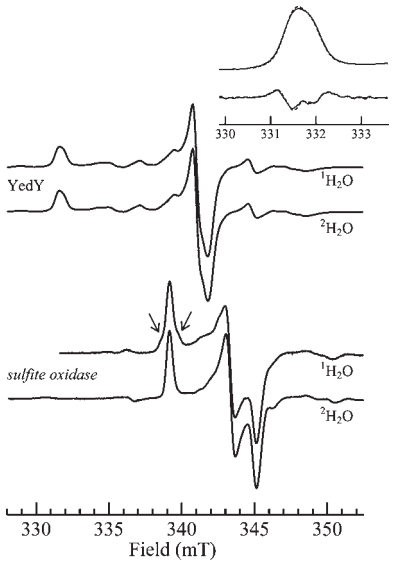

Figure 7. Mo^V EPR spectra of YedY compared with the high-pH spectrum of sulfite oxidase and effects of exchange into a ^2H_2O buffer. The inset compares the g_z region of the YedY spectra (upper traces), together with their second derivatives (lower traces), for ^1H_2O (—) and ^2H_2O (- - -). YedY was enzyme as-isolated with buffer etc., as described in the experimental section; sulfite oxidase was prepared in 100 mM bis-tris-propane/NaOH buffer at pH 9.0 containing 1 mM sulfite to generate the Mo^V oxidation state. The arrows on the ^1H_2O sulfite oxidase high-pH spectrum indicate the ^1H $\Delta m_I = \pm 1$ transitions discussed in the text.

Hamiltonian parameters should be considered as preliminary estimates, and further work using magnetic isotope enrichment and multiple microwave frequencies is required for unambiguous determination.[45] The YedY Mo^V EPR signal also lacks resolved proton splitting from the putative Mo−OH group, which requires some discussion. The high-pH signal of wild-type sulfite oxidase also has no resolved proton hyperfine splitting but, nevertheless, possesses a strongly coupled proton, which was initially detected by observation of formally forbidden $\Delta m_I = \pm 1$ transitions[46] and subsequently by pulsed EPR spectroscopy.[47] Two alternative explanations for the lack of observed splitting have been suggested: that the proton hyperfine tensor from Mo−OH is oriented close to the trimagic angle,[46] where the dipole coupling along each direction of g_x, g_y, and g_z will be zero, or alternatively that the proton splitting was hidden by rotation of the Mo−OH group about the Mo−O bond to yield a static distribution of Mo−O−H orientations and a corresponding ensemble of hyperfine interactions.[47,48] At present, neither of these two alternatives has been definitively proven or disproven for sulfite oxidase, and either phenomenon might be conceivably responsible for the lack of observed proton splitting in the YedY Mo^V EPR spectrum. Alternatively, the presence of substrate and/or product complexes can produce species with no proton coupling,[49] although in these cases, well-defined and discrete Mo^V EPR spectra characteristic of the product or substrate complex are typically observed,[49] so this alternative seems less likely with YedY. Examination of

(42) Harris, H. H.; George, G. N.; Rajagopalan, K. V. *Inorg. Chem.* **2006**, *45*, 493–495.
(43) Allen, F. H.; Kennard, O.; Watson, D. G. *Struct. Correl.* **1994**, *1*, 71–110.
(44) Yang, J.; Rothery, R.; Sempombe, J.; Weiner, J. H.; Kirk, M. L. *J. Am. Chem. Soc.* **2009**, *131*, 15612–15614.
(45) George, G. N.; Bray, R. C. *Biochemistry* **1988**, *27*, 3603–3609.
(46) George, G. N. *J. Magn. Reson.* **1985**, *64*, 384–394.
(47) Astashkin, A. V.; Mader, M. L.; Pacheco, A.; Enemark, J. H.; Raitsimring, A. M. *J. Am. Chem. Soc.* **2000**, *122*, 5294–5302.
(48) Enemark, J. H.; Astashkin, A. V.; Raitsimring, A. M. *J. Chem. Soc., Dalton Trans.* **2006**, 3501–3514.

the YedY Mo^V EPR at high applied microwave powers reveals weak ^1H $\Delta m_I = \pm 1$ transitions, but only of low intensity and consistent with distant protons not directly involved in molybdenum coordination.[46] YedY Mo^V EPR shows some splitting of features, evident in the higher derivative spectra (Figure 7), which might be attributed to ^1H hyperfine splitting; however, exchange into ^2H_2O reveals, at best, only a very subtle sharpening of the features of the spectrum (Figure 7). Thus, this structure is not due to an exchangeable proton and is due to either a nonexchangeable proton or the presence of two different EPR signals with slightly different **g** tensors, which is not unusual among the molybdenum enzymes.[14] The presence of a nonexchangeable Mo−OH might result from reduced water accessibility in the active-site pocket.[9] In any case, definitive determination of whether or not an exchangeable proton is present at the active site must therefore await later experiments using multiple resonance methods.[47,48] Figure 7 also compares the Mo^V high-pH signal of sulfite oxidase showing remarkably different spectra from what have been previously reported as very similar active sites.[11,44]

DFT Calculations and the Active-Site Structure. While EXAFS and EPR provide information on the active-site physical and electronic structures, these techniques, when used in combination with DFT, can provide more definitive information on the active site. A comparison of YedY and sulfite oxidase active-site crystal structures indicates almost identical metal binding sites (Figure 2). The local environment of the molybdenum is, however, significantly different, and Figure 8 shows a comparison of the active sites of sulfite oxidase and YedY. Sulfite oxidase possesses a highly basic active-site pocket adjacent to the active oxygen, bordered by three arginine residues. Arg-138 appears to have a role in catalysis, which may be to transfer substrate/product to and from the active site to the pocket. Other residues thought to be important are also shown in Figure 8. As discussed by Loschi et al.,[11] the active site of YedY lacks these basic groups, which instead has four aromatic residues that make the analogous pocket hydrophobic. Recently combined XAS and DFT of a lethal clinical human mutant sulfite oxidase, in which the arginine closest to Mo Arg-160, equivalent to Arg-138 of the chicken enzyme (Figure 8) is mutated to a glutamine, have shown that O_ε of glutamine provides a donor to the molybdenum of the mutant active site but only in the oxidized Mo^{VI} form.[50] Similarly, the proximity of Asn-45 to the axial coordination site could mean that O_δ of Asn-45 might potentially provide a ligand to a putative oxidized Mo^{VI} site, and we have investigated this possibility with DFT. As we have previously discussed,[50] amides can coordinate metal ions in three different ways—through the $-NH_2$ group of the amide, via a coordinate bond through the carbonyl of the amide, or via formation of the resonance imidic acid [−(HN=)C−OH] form and binding metal through the oxygen—and examples of all three are represented in the Cambridge Structural database.[43]

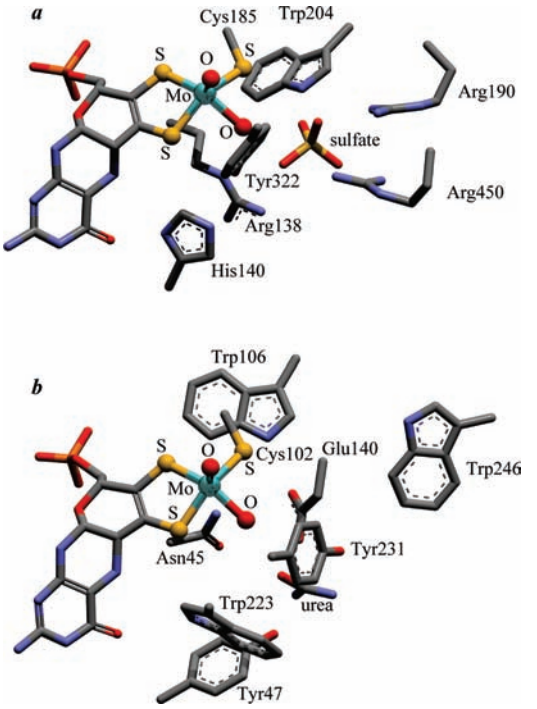

Figure 8. Comparison of sulfite oxidase and YedY active-site structures as determined from protein crystallography: (a) active site determined for chicken sulfite oxidase;[8] (b) active site determined for YedY.[11]

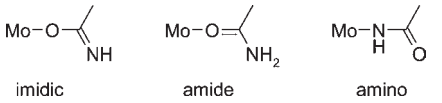

Several different DFT-optimized geometries for the active site were tested for both Mo^V and Mo^{IV} oxidation states. The C_α atoms of amino acid residues were constrained to their crystallographic locations, and only the pyran ring of the molybdenum cofactor was included for computational efficiency. In previous work on sulfite oxidase, both the pyran and amino acid C_α atoms were constrained to crystallographic locations, whereas here the latter constraint was relaxed.[9,51] On the basis of analysis of the EXAFS data discussed above, the Mo^V site can be formulated as an Mo−OH species and the Mo^{IV} site formulated as $Mo-OH_2$. Similar to sulfite oxidase, both Mo^{IV} and Mo^V amino-coordinated complexes were unstable in DFT minimizations and converged to structures in which Asn-45 had dissociated by abstracting a proton from the Mo−OH or $Mo-OH_2$ groups. In the Mo^{IV} oxidation state, Asn-45 oxygen-coordinated alternatives also tended to dissociate from Mo, yielding a five-coordinate active site with a geometry very similar to that determined by protein crystallography, but for Mo^V species, both of these converged to structures where Asn-45 was coordinated via the O_δ

(49) (a) George, G. N.; Prince, R. C.; Kipke, C. A.; Sunde, R. A.; Enemark, J. E. *Biochem. J.* **1988**, *256*, 307–309. (b) Pacheco, A.; Basu, P.; Borbat, P.; Raitsimring, A. M.; Enemark, J. H. *Inorg. Chem.* **1996**, *35*, 7001–7008. (c) George, G. N.; Garrett, R. M.; Graf, T.; Prince, R. C.; Rajagopalan, K. V. *J. Am. Chem. Soc.* **1998**, *120*, 4522–4523. (d) Astashkin, A. V.; Johnson-Winters, K.; Klein, E. L.; Feng, C.; Wilson, H. L.; Rajagopalan, K. V.; Raitsimring, A. M.; Enemark, J. H. *J. Am. Chem. Soc.* **2008**, *130*, 8471–8480.

(50) Doonan, C. J.; Wilson, H.; Garrett, R. M.; Bennet, B.; Prince, R. C.; Rajagopalan, K. V.; George, G. N. *J. Am. Chem. Soc.* **2007**, *129*, 9421–9428.

(51) Qiu, J. A.; Wilson, H. L.; Pushie, M. J.; Kisker, C.; George, G. N.; Rajagopalan, K. V. *Biochemistry* **2010**, *49*, 3989–4000.

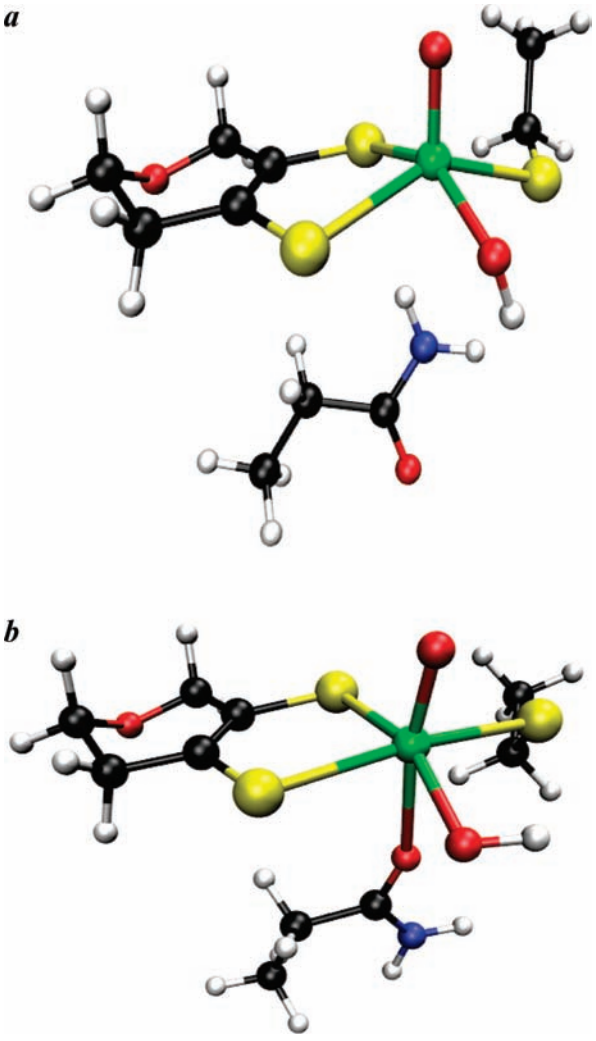

Figure 9. DFT-optimized structures for the MoV form of the YedY active site, with the Asn45 side chain oriented as implicated in the crystal structure (a) and with the side chain reoriented with the O_δ atom bound to the Mo center (b).

atom, with amide-coordinated species typically having longer bond lengths than imidic coordination. In previous work, DFT calculations of R160Q sulfite oxidase gave Mo^V structures where Gln-160 was bound via imidic coordination;[50] however, YedY did not do this unless constraints on the pyran location were relaxed; in which case, Asn-45 O_δ was coordinated approximately trans to the Mo=O group with a Mo−O_δ(Asn-45) amide bond length of 2.56 Å, which is very close to the long-distance light atom observed by EXAFS (Table 1 and Figure 5). Selected DFT energy-minimized structures are shown in Figure 9, and selected bond lengths and angles are given in Table 2. This suggests the possibility of a six-coordinate pseudooctahedral active site where Asn-45 provides an O-donor atom to molybdenum in the Mo^V but not in the Mo^{VI} oxidation state. An alternative source of the long Mo−O EXAFS might be a coordinated water (Mo−OH_2); however, DFT calculations including a distal water ligand tended to converge to structures in which H_2O was dissociated from the metal, and we therefore consider this possibility less likely. In some calculations, Tyr-231 was included (again with C_α constrained at the crystallographic location) and allowed to rotate so that its O atom could

Table 2. Selected Interatomic Distances[a] for DFT-Computed Structures versus Crystallography

bond	six-coordinate Mo^V	five-coordinate Mo^V	Mo^{IV}	crystallography[b]
Mo−O_1	1.688	1.697	1.700	1.7
Mo−O_2	1.985	1.968	2.233	2.2
Mo— S_1'	2.464	2.437	2.416	2.4
Mo— S_2'	2.482	2.435	2.393	2.4
Mo−S_γ(C102)	2.505	2.441	2.424	2.5
Mo−O_δ(N45)	2.562			

[a] Interatomic distances are given in angstroms and are specified to the precision of the convergence criteria used for the energy minimization. DFT tends to give systematically different bond lengths (generally shorter) but, in most cases, is expected to be within 0.05 Å, although relative bond lengths will be more accurate than this. [b] Values taken from the coordinates deposited in the protein structure database.[11]

Table 3. Comparison of Experimental[a] and Computed Mo^V EPR g Values

	g_x	g_y	g_z	g_{ave}
high-pH sulfite oxidase	1.953	1.964	1.987	1.968
YedY	1.969	1.974	2.030	1.991
DFT, five-coordinate	1.970	1.974	1.993	1.979
DFT, six-coordinate	1.950	1.969	2.012	1.977

[a] Experimental g values were obtained by computer simulation (not illustrated) as described in the Materials and Methods section.

hydrogen bond with the Mo−OH group; in these calculations, the Mo−OH group adopted a different orientation, and we conclude that the overall structure of the molybdenum site can be highly dependent on the protein. Using the Mo−S bond lengths from DFT and eq 3 gives a σ_{stat}^2 value of 0.0003 $Å^2$, which agrees well with our estimate from EXAFS of 0.0004 $Å^2$.

The fact that a six-coordinate site was not observed in the crystal structure can be explained by photoreduction of the active site. Photoreduction is a very common problem in the crystallography of metalloprotein systems.[52] For sulfite oxidase, almost all crystal structures reported to date have photoreduced molybdenum sites (probably Mo^{IV}) because of the large X-ray dose required for crystallographic data acquisition.[52] Indeed, the only reports of oxidized sulfite oxidase crystal structures are the C185S and C185A mutants,[51] both of which contain trioxo active sites,[18,51,52] which are very difficult to reduce.[53] Thus, by analogy with other molybdenum enzymes, it seems likely that the YedY crystal structure is of photoreduced enzyme in the Mo^{IV} state, which is consistent with both our XAS and DFT analysis. The novel six-coordinate Mo^V active site also provides a potential explanation for the unusual Mo^V EPR of YedY because *pseudo*-octahedral coordination will effectively raise the donor orbitals of the dithiolene ligand into the plane of the half-occupied ground-state Mo $4d_{xy}$ orbital, facilitating spin delocalization onto the dithiolene sulfur ligands through spin−orbit coupling, giving rise to the high observed g_z value. To test this possibility, we conducted DFT calculations of g values, which are compared with experimental values in Table 3, computed using the

(52) George, G. N.; Pickering, I. J.; Kisker, C. *Inorg. Chem.* **1999**, *38*, 2539–2540.
(53) George, G. N.; Garret, R. M.; Prince, R. C.; Rajagopalan, K. V. *Inorg. Chem.* **2004**, *43*, 8456–8460.

coordinates of Figure 9. We found that, in general, DFT gave g values that were very sensitive to quite subtle changes in the molybdenum coordination. Nevertheless, the trend is for somewhat higher g_z values in the six-coordinate structures, but the changes are more subtle than those observed experimentally. We conclude that the YedY Mo^V EPR spectra are consistent with those of the six-coordinate site but that no definitive conclusions can be made on the basis of these data alone.

In summary, we conclude that the Mo^V oxidation state of YedY possesses a six-coordinate active site, with Asn-45 O_δ possibly providing a distant ligand to the molybdenum, located trans to the Mo=O group. DFT calculations using this geometry adequately reproduce the unusual EPR of YedY. The Mo^{IV} YedY site is five-coordinate and very similar to the sulfite oxidase active site. The active site of YedY thus exhibits significant similarities to but also some remarkable differences from other members of the sulfite oxidase family of molybdenum enzymes. The widespread occurrence of YedY in pathogenic organisms makes the enzyme of significant interest, but many open questions remain concerning its physiological function and how its unique structural features relate to this. In this regard, it remains arguably the most intriguing member of the sulfite oxidase family of molybdenum enzymes.

Acknowledgment. Portions of this work were carried out at the Stanford Synchrotron Radiation Laboratory, which is funded by the U.S. Department of Energy, Office of Basic Energy Sciences and Office of Biological and Environmental Sciences, and the National Institutes of Health, National Center for Research Resources. Research at the University of Saskatchewan was supported, in part, by a Canada Research Chair award (GNG), the University of Saskatchewan, the Province of Saskatchewan, and the Natural Sciences and Engineering Research Council (Canada). M.J.P. is a Canadian Institutes for Health Research - Training in Health Research Using Syhchrotron Techniques (CIHR-THRUST) Fellow. Research at the University of Alberta was supported by the Canadian Institutes of Health Research. We thank Nasim Boroumand for help with the YedY purification. This research has been enabled by the use of WestGrid computing resources, which are funded, in part, by the Canada Foundation for Innovation, Alberta Innovation and Science, BC Advanced Education, and the participating research institutions. WestGrid equipment is provided by IBM, Hewlett-Packard, and SGI.